Ab initio lattice dynamics of sapphire

R. Heid
Institut für Theoretische Physik, Universität Regensburg, D-93049 Regensburg, Germany
and Forschungszentrum Karlsruhe, Institut für Festkörperphysik, P.O. Box 3640, D-76021 Karlsruhe, Germany

D. Strauch
Institut für Theoretische Physik, Universität Regensburg, D-93049 Regensburg, Germany

K.-P. Bohnen
Forschungszentrum Karlsruhe, Institut für Festkörperphysik, P.O. Box 3640, D-76021 Karlsruhe, Germany
(Received 29 October 1999)

Structural and lattice dynamical properties of sapphire are investigated within the framework of density-functional perturbation theory. We obtain weak anisotropies in the dielectric tensor and in the Born effective charges. The theoretical phonon dispersions are found to be in very satisfactory agreement with available experimental data.

Sapphire (α-Al_2O_3) belongs to the class of aluminum oxides which are very common materials in the earth's crust. Due to its outstanding mechanical and optical properties, sapphire finds a wide range of technological applications, e.g., in catalytic and corrosion technology, or as substrate material. Its importance has motivated a variety of theoretical investigations aimed to elucidate its underlying electronic and binding properties. While the electronic structure of sapphire is now well understood on the basis of *first principles* calculations,[1,2] its lattice dynamics has only been studied in the context of phenomenological models adjusted to optical and neutron scattering data.[3,4]

In this paper, we present an investigation of the lattice dynamics of sapphire in the framework of density-functional theory. This is achieved by combining a mixed-basis pseudopotential approach,[5] which allows an efficient treatment of the stronger localized O-like valence states, with modern density-functional perturbation theory.[6,7]

Calculations are performed within the local-density approximation (LDA) using the Hedin-Lundqvist form of the exchange-correlation functional.[8] We employ norm-conserving pseudopotentials of the Hamann-Schlüter-Chiang type.[9] The valence states are represented by four local functions of s and p type at each oxygen site, smoothly cut off at a radius of 1.3 a.u., and plane waves up to a kinetic energy of 20 Ry. Brillouin-zone (BZ) sampling in the band-structure calculation was performed on a $4\times4\times4$ simple rhombohedral k-point mesh corresponding to 13 special points in the irreducible wedge of the BZ.

TABLE I. Bulk properties of sapphire. Experimental values are taken from Ref. 16. The all-electron calculation from Boettger (Ref. 2) employs Gaussian-type basis functions.

	a(Å)	c/a	v	u	B (MBar)	dB/dP
Mixed basis	9.57	2.733	0.102	0.307	2.45	4.0
Experiment	9.71	2.730	0.102	0.306	2.54	4.3
All electron	9.68	2.721	0.102	0.306	2.44	4.3

The lattice structure of sapphire (α-Al_2O_3) belongs to the trigonal system (space group $R\bar{3}c$). Its rhombohedral unit cell contains 2 formula units (10 atoms). The structure can be viewed as a slightly distorted hexagonal close-packed lattice of oxygen ions, where the aluminum ions occupy 2/3 of the octahedral interstices, and is determined by four parameters: the rhombohedral lattice constant and angle, or, alternatively, the hexagonal lattice constants a and c, and two internal parameters u and v describing the positions of the O and Al ions, respectively.[10]

The static equilibrium structure is found in the following way. For fixed volume V, the total energy E is minimized with respect to the internal parameters (u and v) and the ratio c/a. Repeating this for a set of different volumes, the optimal volume is then determined from a fit of $E_{\min}(V)$ to the Murnaghan equation of state. Finally, the parameters u, v, and c/a are optimized again. Results of this procedure are summarized in Table I. The internal parameters and the c/a ratio are found in excellent agreement with experimental values. Small deviations of the lattice constant (-1.4%) and bulk modulus (-3.7%) are typical for LDA. Our results are also in accord with a recent all-electron LDA calculation,[2] confirming the adequacy of our pseudopotential approach.

Phonon properties are calculated using density-functional perturbation theory. This efficient approach originally formu-

TABLE II. Theoretical values for the screened Born-effective charge tensors $Z_{\alpha\beta}/\sqrt{\epsilon^{\infty}_{zz}}$. Values given for O correspond to the ion with rhombohedral coordinates $(\frac{1}{4}-u,\frac{1}{4},-\frac{1}{4}+u)$. For all Al ions charge tensors are equal by symmetry.

	Al			O		
	x	y	z	x	y	z
x	1.65	0	0	−1.15	0	0
y	0	1.65	0	0	−1.04	−0.14
z	0	0	1.63	0	−0.19	−1.09

TABLE III. Calculated properties of infrared-active modes. Frequencies are given in THz. The third quantity is a measure for the oscillator strength. Here, $\alpha=z$ or $\alpha=x,y$ for A_{2u} or E_u modes, respectively. Experimental values (in brackets) are taken from Ref. 13.

	ν_{TO}	ν_{LO}	$\Delta\epsilon_{\alpha\alpha}/\epsilon^{\infty}_{\alpha\alpha}$
A_{2u}	11.72 (12.0)	14.98 (15.4)	2.23 (2.19)
	17.14 (17.5)	25.79 (26.1)	0.51 (0.55)
E_u	11.44 (11.6)	11.50 (11.6)	0.06 (0.09)
	13.05 (13.3)	14.41 (14.4)	0.92 (0.84)
	16.95 (17.1)	18.74 (18.8)	0.99 (0.94)
	18.83 (19.1)	26.60 (27.0)	0.04 (0.09)

lated for a plane-wave expansion of the valence states[6,7] has been recently extended to general nonorthogonal basis sets suitable for the use of a mixed-basis representation (for details of the formalism see Ref. 11). As sapphire is an insulator, a complete characterization of its lattice dynamics requires knowledge of the dielectric tensor $\epsilon^{\infty}_{\alpha\beta}$ and Born effective-charge tensors $Z^{*}_{\alpha\beta}(\kappa)$ for each ion κ, which determine the nonanalytic contribution to the dynamical matrix in the limit $q\rightarrow 0$.[7,12] Currently, a perturbative approach to these quantities has not been implemented for the mixed-basis scheme. We therefore pursued the alternative way of extracting the nonanalytic part from calculations for q points close to the center of the BZ along three different directions in reciprocal space. By this procedure, all matrix elements of the dielectric and Born effective-charge tensors can be determined except for a single scale factor because only ratios $Z^{*}/\sqrt{\epsilon^{\infty}}$ enter the expression for the dynamical matrix.

In trigonal symmetry, the dielectric tensor is diagonal and has only two independent elements $\epsilon_{xx}=\epsilon_{yy}$ and ϵ_{zz}. We find a small anisotropy $\epsilon_{xx}/\epsilon_{zz}=1.02$ in agreement with measurements [$\epsilon_{xx}=3.2$, $\epsilon_{zz}=3.1$ (Ref. 13)]. Independent elements of the Born effective-charge tensors are shown in Table II. For both ion species, results indicate only small anisotropies, being largest for the O ions which occupy sites of low C_2 symmetry.

Calculated frequencies of Γ-point phonons are summarized in Tables III and IV. Comparison of infrared (IR) and Raman active modes with optical data gives a maximum deviation of 2.7%.[13,14] In case of the IR modes, information about the accuracy of the theoretical eigenvectors $\eta^{\mathrm{TO}}(\lambda)$ of mode λ can be gained from the contribution $\Delta\epsilon(\lambda)$ of each mode to the total static dielectric tensor $\epsilon^{0}_{\alpha\beta}=\epsilon^{\infty}_{\alpha\beta}+\Sigma_{\lambda}\Delta\epsilon_{\alpha\beta}(\lambda)$, given by[15]

TABLE IV. Frequencies of the Raman-active (A_{1g}, E_g) and silent (A_{2g}, A_{1u}) modes in THz. Experimental values for Raman-active modes (in brackets) are taken from Ref. 14.

A_{1g}	E_g	A_{2g}	A_{1u}
12.34 (12.5)	11.38 (11.3)	9.04	17.82
19.07 (19.4)	12.86 (13.0)	16.08	20.62
	13.27 (13.5)	22.41	
	17.02 (17.3)		
	22.38 (22.5)		

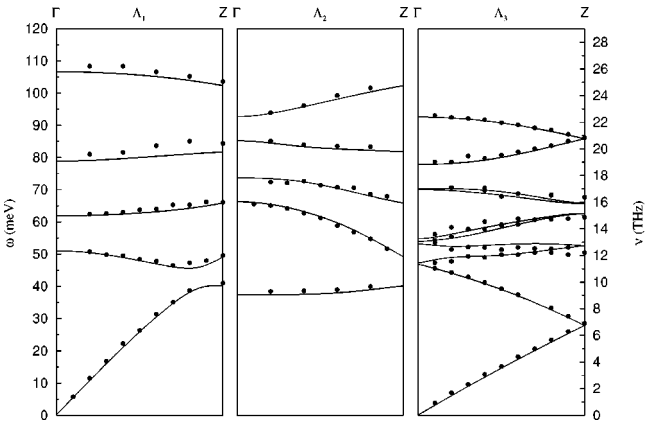

FIG. 1. Phonon dispersions of sapphire along the Γ-Z direction (rhombohedral axis), given separately for each of the three irreducible representations. Lines are theoretical results, and dots represent neutron-scattering data of Ref. 4.

$$\Delta\epsilon_{\alpha\beta}(\lambda)=\frac{4\pi}{V\omega^{2}_{\mathrm{TO}}(\lambda)}m_{\alpha}(\lambda)m_{\beta}(\lambda). \tag{1}$$

Here, V is the volume of the elementary cell, $\omega_{\mathrm{TO}}(\lambda)$ is the transverse frequency of the mode, and $\mathbf{m}(\lambda)$ is the induced electric moment of the elementary cell per unit displacement. The latter quantity is related to the Born effective charges and the mode eigenvectors by

$$m_{\alpha}(\lambda)=\sum_{\kappa\beta}Z^{*}_{\alpha\beta}(\kappa)\frac{\eta^{\mathrm{TO}}_{\kappa\beta}(\lambda)}{\sqrt{M_{\kappa}}}, \tag{2}$$

where M_{κ} denotes the mass of ion κ. For the trigonal lattice, $\Delta\epsilon_{\alpha\beta}(\lambda)$ is again diagonal, with nonzero matrix elements $\Delta\epsilon_{zz}$ for modes having induced polarization parallel to the rhombohedral symmetry axis (A_{2u} representation), and nonzero $\Delta\epsilon_{xx}$, $\Delta\epsilon_{yy}$ for those with induced polarization perpen-

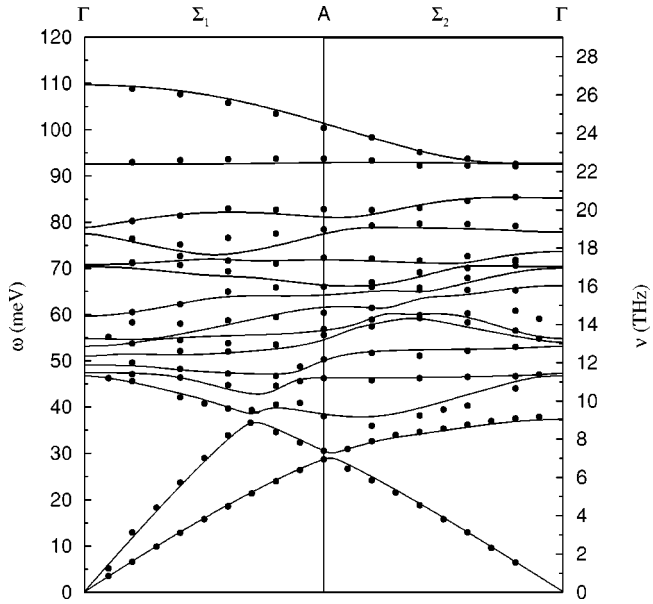

FIG. 2. Same as Fig. 1, but for the Γ-A direction [$A=(0,0.5,0)$]. For clarity, the two irreducible representations have been unfolded.

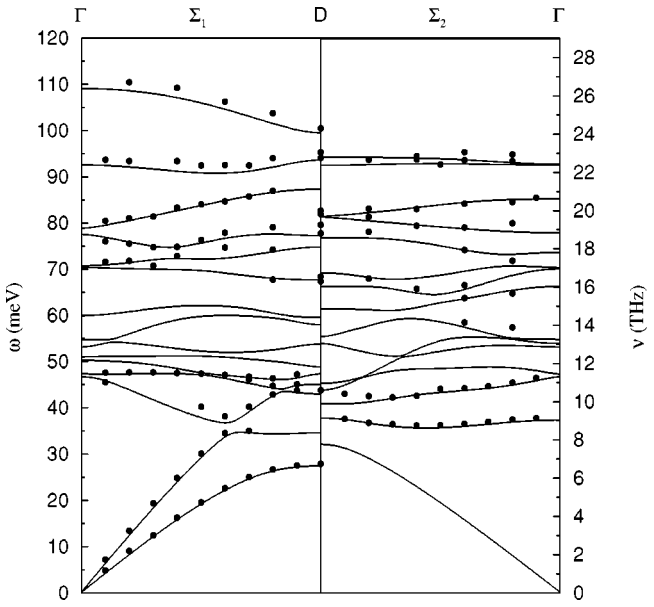

FIG. 3. Same as Fig. 1, but for the Γ-D direction [$D=(0.5,0,0.5)$]. For clarity, the two irreducible representations have been unfolded.

dicular to this axis (E_u). Table III shows theoretical values for the ratio $\Delta\epsilon_{\alpha\alpha}(\lambda)/\epsilon^{\infty}_{\alpha\alpha}$. They agree with experimental data better than 10% for modes with strong infrared activity demonstrating that the present calculation also provides realistic eigenvectors.

To obtain the complete phonon spectrum we have determined the dynamical matrices on a $4\times4\times4$ mesh, which is then extended to the whole BZ using a standard Fourier interpolation technique.[7,12] In Figs. 1, 2, and 3, dispersion curves are shown along three high-symmetry directions for which neutron scattering experiments have been performed. The theoretical dispersion curves compare very favorably with experiment and provide predictions for those phonon branches along the Γ-D direction which have not been measured so far. The prominent features of the phonon density of states, shown in Fig. 4, are pseudogap structures near 43 and 87 meV, and a strong peak near 92 meV which is due to a nearly dispersionless oxygen mode.

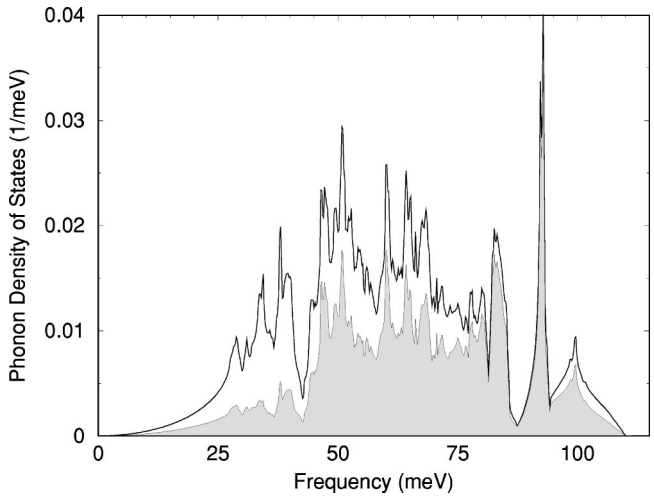

FIG. 4. Theoretical phonon density of states of sapphire. The shaded area denotes the partial density of states of the oxygen ions.

In summary, we have presented results from a DFT based investigation of the structural and lattice dynamical properties of sapphire. We find an excellent agreement with the measured phonon spectra, demonstrating that the perturbative approach applied in this work can provide very accurate predictions of the lattice dynamics of metal oxides with nontrivial crystal structures.

Financial support by the Deutsche Forschungsgemeinschaft (Graduiertenkolleg Komplexität in Festkörpern: Phononen, Elektronen und Strukturen, GRK 176/3) is gratefully acknowledged. We would also like to thank the Landesrechenzentrum in Munich for granting us Fujitsu VPP700 computing time.

[1] W.Y. Ching and Y.N. Xu, J. Am. Ceram. Soc. **77**, 404 (1994).
[2] J.C. Boettger, Phys. Rev. B **55**, 750 (1997).
[3] W. Kappus, Z. Phys. B **21**, 325 (1975).
[4] H. Schober, D. Strauch, and B. Dorner, Z. Phys. B: Condens. Matter **92**, 273 (1993).
[5] S.G. Louie, K.M. Ho, and M.L. Cohen, Phys. Rev. B **19**, 1774 (1979).
[6] S. Baroni, P. Giannozzi, and A. Testa, Phys. Rev. Lett. **58**, 1861 (1987).
[7] P. Giannozzi, S. de Gironcoli, P. Pavone, and S. Baroni, Phys. Rev. B **43**, 7231 (1991).
[8] L. Hedin and B.I. Lundqvist, J. Phys. C **4**, 2064 (1971).
[9] D.R. Hamann, M. Schlüter, and C. Chiang, Phys. Rev. Lett. **43**, 1494 (1979); G.B. Bachelet, D.R. Hamann, and M. Schlüter, Phys. Rev. B **26**, 4199 (1982).
[10] The rhombohedral bravais vectors are given by $\mathbf{a}_1=(a/2, -\sqrt{3}a/6, c/3)$, $\mathbf{a}_2=(0, a/\sqrt{3}, c/3)$, and $\mathbf{a}_3=(-a/2, -\sqrt{3}a/6, c/3)$, where a and c are the hexagonal lattice constants. Choosing the inversion center at the origin, the rhombohedral coordinates of the ions are $(\frac{1}{4}-u, \frac{1}{4}, -\frac{1}{4}+u)$ and $(\frac{1}{4}+v, \frac{1}{4}+v, \frac{1}{4}+v)$ for O and Al, respectively, with u and v being the free structural parameters. The positions of the remaining 8 ions are determined by lattice symmetry.
[11] R. Heid and K.-P. Bohnen, Phys. Rev. B **60**, R3709 (1999).
[12] X. Gonze and C. Lee, Phys. Rev. B **55**, 10 355 (1997).
[13] A.S. Barker, Jr., Phys. Rev. **132**, 1474 (1963).
[14] S.P.S. Porto and R.S. Krishnan, J. Chem. Phys. **47**, 1009 (1963).
[15] A.A. Maradudin, in *Dynamical Properties of Solids*, edited by G. K. Horton and A.A. Maradudin (North Holland Publishing, Amsterdam, 1974), Vol. 1, p. 1.
[16] H. d'Amour, D. Schiferl, W. Denner, H. Schulz, and W.B. Holzapfel, J. Appl. Phys. **49**, 4411 (1978).